



High-Temperature Mechanical Properties and Microstructure of High Belite Cement

Wu Zhiqiang^{1,2*}, Xie Renjun², Yang Jin¹, Ni Xiucheng^{3,4} and Cheng Xiaowei^{3,4*}

¹School of Safety and Ocean Engineering, China University of Petroleum (Beijing), Beijing, China, ²CNOOC Research Institute Co. Ltd., Beijing, China, ³School of New Energy and Materials, Southwest Petroleum University, Chengdu, China, ⁴State Key Laboratory of Oil and Gas Reservoir Geology and Exploitation, Southwest Petroleum University, Chengdu, China

OPEN ACCESS

Edited by:

Hanfeng Liang,
Xiamen University, China

Reviewed by:

Yizhou Zhang,
Nanjing University of Information
Science and Technology, China
Jiapei Du,
RMIT University, Australia

*Correspondence:

Wu Zhiqiang
chengxw@swpu.edu.cn
Cheng Xiaowei
chengxw@swpu.edu.cn

Specialty section:

This article was submitted to
Energy Materials,
a section of the journal
Frontiers in Materials

Received: 09 December 2021

Accepted: 17 January 2022

Published: 02 February 2022

Citation:

Zhiqiang W, Renjun X, Jin Y,
Xiucheng N and Xiaowei C (2022)
High-Temperature Mechanical
Properties and Microstructure of High
Belite Cement.
Front. Mater. 9:831889.
doi: 10.3389/fmats.2022.831889

The use of the class G oil well cement for cementing in high-temperature deep-seated oil and gas wells declines its mechanical properties, which limit its application under high-temperature conditions. The high belite cement (HBC), a new class of energy-saving and environmentally friendly cement, has been widely used in recent years. In this study, the mechanical properties, phase composition and microstructure of HBC and quartz sand have been analyzed at high temperature, so as to optimize the amount of sand and provide guidelines for further exploring the application of HBC in the high-temperature oil and gas well cementing. The experimental results show that the high-temperature mechanical properties of the cement stone mixed with 40% quartz sand are the highest, thus, delaying the decline in the strength to the greatest extent. The microscopic analysis reveals that HBC produces dicalcium silicate hydrate and hydroxyl silicon calcium stone at high temperature. On mixing the quartz sand, xonotlite is observed to appear in the cement hydrate phase. These products are observed to be small in size and dense in structure, thus, leading to a delay in the decline of the high-temperature mechanical properties of the cement stone.

Keywords: high belite cement, quartz sand, microstructure, high temperature, mechanical properties

INTRODUCTION

Currently, the petroleum exploration and exploitation technologies are becoming more mature, and the exploitation is gradually advancing to the deep and ultra-deep wells (Vidal et al., 2018; Guo et al., 2019; Kuzielová et al., 2019). At present, the temperature of the deep wells can reach up to 110–150°C (Wang et al., 2019), whereas the temperature of the ultra-deep wells can reach above 200°C (Bu et al., 2016; Vidal et al., 2018; Guo et al., 2020). Under such working conditions, the mechanical properties of the conventional class G cement systems are significantly deteriorated and cannot meet the cementing quality requirements (Wei et al., 2021).

Reducing the calcium to silicon ratio in the cement materials is an effective strategy to overcome the significant deterioration in the performance of the class G oil well cement at high temperatures. The currently used high belite cement (HBC) (Cuesta et al., 2021) consists of C₂S as the dominant mineral component. The CaO/SiO₂ molecular ratio in this cement material is significantly higher than that of the class G oil well cement, thus, retaining the high temperature cement strength to a certain extent (Jiang et al., 2021a). The clinker system of HBC can be easily grinded and possesses a low firing temperature (Koumpouri et al., 2021). It also exhibits significant advantages such as low heat of hydration and high later strength (Sui et al., 2015; Cuesta et al., 2021). In terms of the

TABLE 1 | HBC chemical composition and percentage content.

Composition	Loss	SiO ₂	Al ₂ O ₃	Fe ₂ O ₃	CaO	MgO	SO ₃	Total
Content/%	0.56	22.88	4.26	4.71	62.42	1.52	2.43	98.78

TABLE 2 | HBC mineral composition and percentage content.

Composition	KH	N	P	C ₃ S	C ₂ S	C ₃ A	C ₄ AF	C ₄ AF+2C ₃ A
Content/%	0.812	2.55	0.9	37.87	36.97	3.3	14.32	20.92

Notes: KH: lime saturation factor. Indicates the degree to which silica oxide in the clinker is saturated with calcium oxide to produce tricalcium silicate.

N: silica rate (Also known as silicic acid rate). It represents the mass ratio of silica content to alumina and iron oxide in the clinker, and also represents the ratio of silicate minerals to solvent minerals in the clinker.

P: Aluminum rate (Also known as aluminum oxygen rate). It represents the mass ratio of alumina and iron oxide content in the clinker, and also represents the ratio of tricalcium aluminate to tetracalcium aluminate ferrite in the clinker solvent mineral.

C₃S: 3CaO·SiO₂, tricalcium silicate.

C₂S: 2CaO·SiO₂, dicalcium silicate.

C₃A: 3CaO·Al₂O₃, tricalcium aluminate.

C₄AF: 4CaO·Al₂O₃·Fe₂O₃, tetracalcium aluminoferrite.

production technology, HBC, as a new type of environmentally friendly cement material with low energy consumption and low emissions, is of high significance for the energy conservation and emission reduction, thereby realizing the national policies of “carbon peak” and “carbon neutrality”.

In the current research, some scholars have developed Belite sulphoaluminate cement (Gong and Fang, 2016). However, its high sulfur content limits its application, and the cement can only be used under a few specific working conditions. In addition, the literature studies have shown that the curing temperature (Bahafid et al., 2017) and type of the doping cations also affect the performance of HBC (Jiang et al., 2021b; Shirani et al., 2021); At the same time, the hydration rate of HBC is significantly accelerated at high temperatures, which can effectively improve its early strength. Thus, at present, the quartz sand is still used for compounding at high temperatures (Li et al., 2016; Liu et al., 2021). However, HBC is currently rarely used in high-temperature deep wells, with a majority of the wells still using the class G oil well cement slurry system. In addition, HBC lacks a mature system under high temperature conditions (above 200°C), along with a lack of systematic research on its application in the high-temperature deep wells.

This study analyzes the chemical and mineral compositions of HBC to study the influence of the quartz sand on its slurry and high temperature performances. In addition, XRD, TG, SEM, BET and other micro-testing methods have been used to explore the phase composition and microstructure of the cement stone, thereby analyzing the mechanism of strength change, so as to provide guidelines for the high-temperature deep well cementing.

EXPERIMENTAL

Raw Materials

- 1) High belitec (HBC): provided by Jiahua Special Cement Co. Ltd. Its chemical composition and mineral composition are presented in **Table 1** and **Table 2**.
- 2) Quartz sand: provided by Henan Weihui Chemical Co. Ltd.

The particle size distribution of HBC and quartz sand is shown in **Figure 1**.

As per **Figure 1**, the median particle size can be obtained as: dHBC (0.5) = 43.230 μm and d quartz sand (0.5) = 46.407 μm. It can be observed that the average particle size of the two materials is relatively close, thus, leading to a superior particle gradation and effective dispersion during the preparation of the cement slurry, thereby ensuring the sedimentation stability of the slurry.

- 3) Additives: mainly fluid loss agent G33S and dispersant SXY-2, provided by Henan Weihui Chemical Co. Ltd.

Experimental Methods

Sample Preparation and Curing

The cement slurry was prepared by following the GB/T 19139-2012 “Oil Well Cement Test Method” (Standard C N. GB/T 19139-2012, 2012) and API RP 10B standards “Oil Well Cement Material and Experiment Specification” (Institute A P. API RP 10B-2, 2013). The performance of the cement slurry was tested referring to GB/T 10238-2015 “Oil Well Cement” (Standard C N. GB/T 10238-2015, 2015). The cement slurry was poured into a 50.8*50.8*50.8 square mold and placed in a water bath at 30°C, 50°C, 70°C and 90°C for curing for 1, 3 and 7 d. The high temperature curing experiment of the cement stone was carried out in a specialized high-temperature and high-pressure curing kettle. The curing temperatures were 110°C, 150°C, 180°C and 220°C, and the curing duration was 7 d.

Sample Testing and Analysis

Use TY-300 pressure testing machine to test its compressive strength. The loading rate is 2 kN/min ± 0.2 kN/min. The phase composition of cement stone is tested by dx-2000 X-ray diffractometer (Dandong Haoyuan Instrument Co., Ltd.): The test angle range is 5–70°, the pace is 0.04°/s, and the test equipment voltage and current are 30 kV and 20 mA, respectively. The micro morphology of the cement stone was tested with ZEISS EV0 MA15 scanning electron microscope (Carl

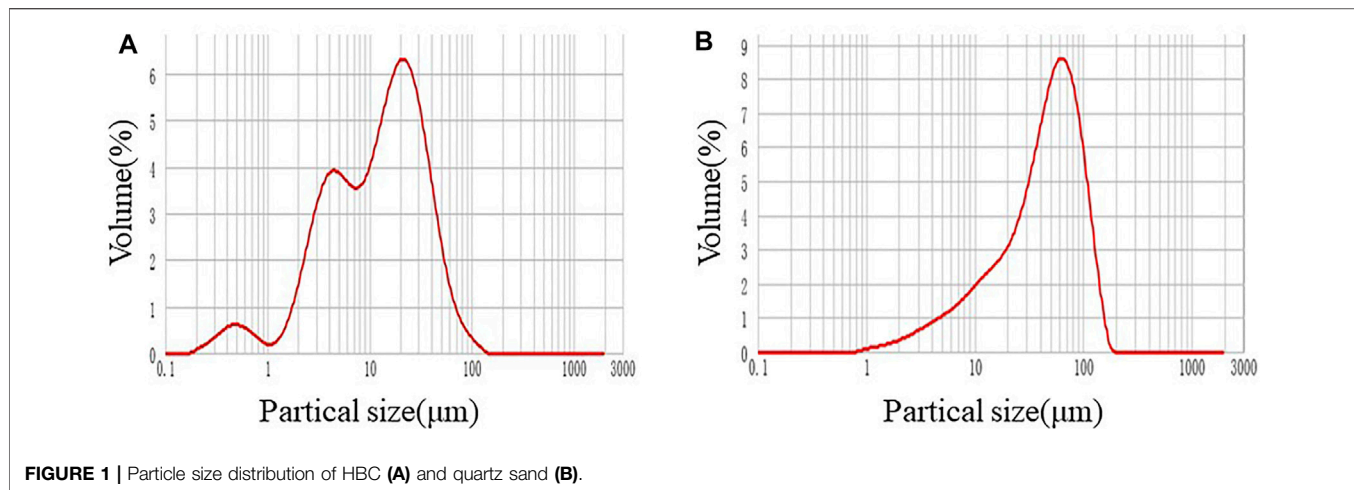


FIGURE 1 | Particle size distribution of HBC (A) and quartz sand (B).

TABLE 3 | The HBC slurry properties.

ID	Cement (%)	Quartz sand (%)	Density (g/cm ³)	Liquidity (cm)	Fluidity index(n)	Consistency coefficient (K(Pa.s ⁿ))	Sedimentation stability/ $\Delta psc/\%$		
							Top	Middle	Bottom
B-0	100	0	1.93	23.50	0.82083	0.65720	100	100	100
B-10	100	10	1.92	23.00	1.02953	0.17884	100	100	100
B-20	100	20	1.90	22.70	0.9534	0.28751	99.9	99.9	100.1
B-30	100	30	1.89	22.40	1.081459	0.12936	99.9	99.9	100.1
B-40	100	40	1.89	21.90	0.92272	0.31251	99.9	99.9	100.2
B-50	100	50	1.86	19.50	0.87132	0.43673	99.8	99.9	100.2

Zeiss, Germany): Resolution: high vacuum mode, 3.0 nm (30 kV); magnification: 5X-300000X; acceleration voltage: 0.3–30 kV. S8 TIGER X-ray fluorescence spectrometer (Bruck AXS, Germany) was used to test the mineral composition and chemical composition of the samples at 25°C, with an applicable power supply of 380 V \pm 10%, a frequency of 50 HZ, and an external argon supply with a purity of 99.999%. An external UPS power supply was utilized in order to prevent sudden power failures and damages to the instrument. The F-Sorb 3,400 specific surface area and pore size analyzer (BET) was used to measure the pore size of the cement stone. The principle of the test is that at the temperature of liquid nitrogen, the amount of nitrogen adsorbed on the surface of the cement stone pores depends on the ratio of the nitrogen partial pressure P and the saturated vapor pressure P0 of nitrogen at the liquid nitrogen temperature (P/P0). When P/P0 \geq 0.4, capillary aggregation will occur, so that the pore size distribution of cement stone can be measured.

RESULTS AND DISCUSSION

Engineering Performance of HBC Slurry

A large amount of external admixtures affects the basic engineering performance of the cement paste to a certain extent, even affecting the construction in severe cases. The

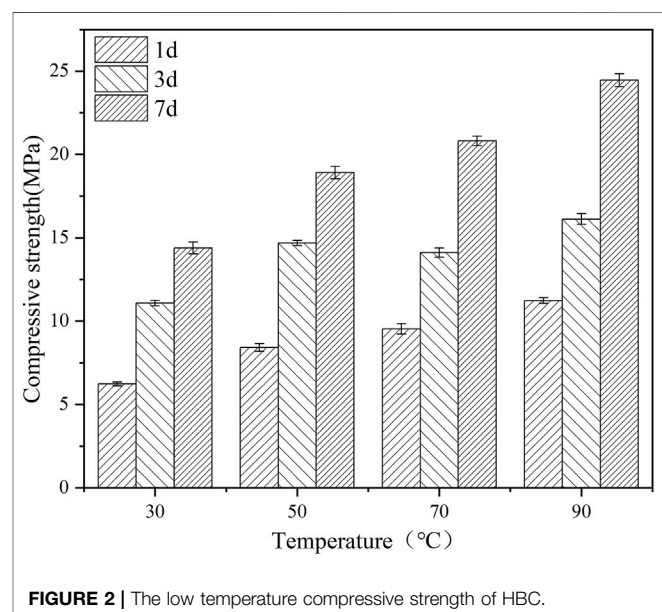
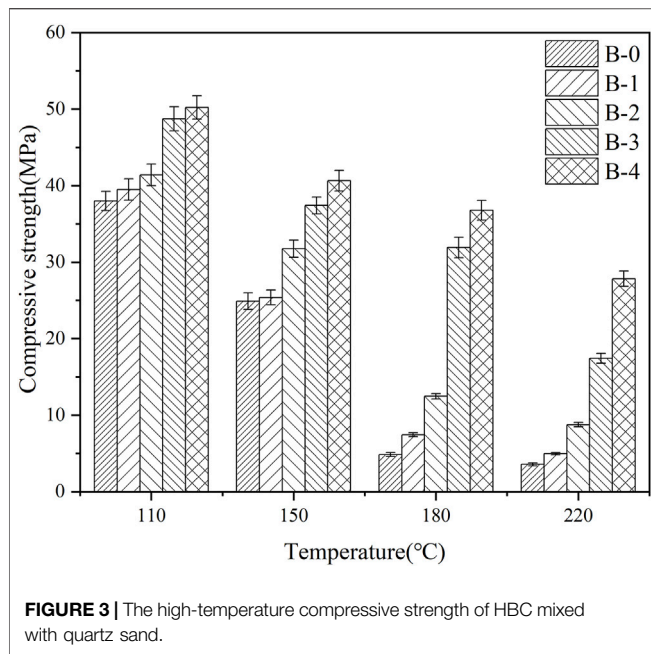


FIGURE 2 | The low temperature compressive strength of HBC.

content of quartz sand is set in this study as 0, 10, 20, 30, 40 and 50%. The amount of the fluid loss agent is 1%, whereas the dispersant amount is 0.5%, both of which are the mass percentages of HBC. Further, the water-solid ratio is 0.44.



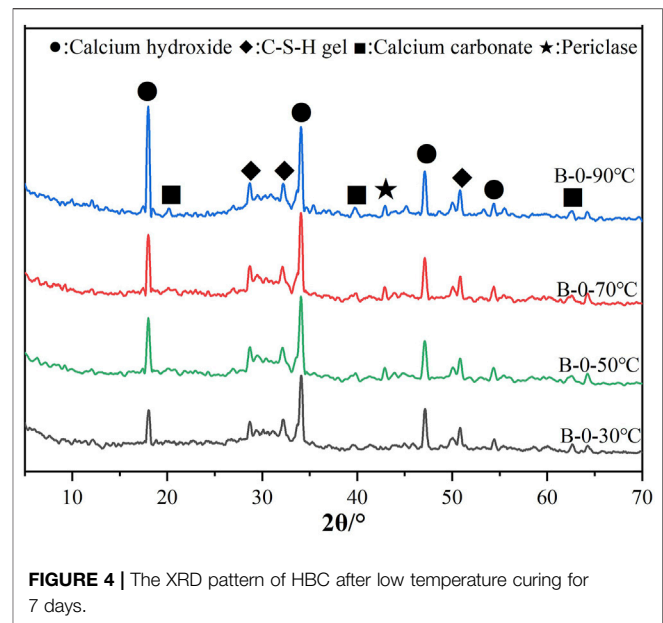
The properties of the tested cement paste are shown in **Table 3**.

It can be observed from the experimental data that increasing the amount of the quartz sand gradually decreases the density of the cement slurry. In addition, the liquidity, fluidity and consistency coefficient of the cement slurry are in excellent condition. The settlement stability of cement slurry is excellent. Taking into account the performance and cost of the slurry as well as the mixing ratio of the external admixtures, the amounts of quartz sand are determined to be 0, 10, 20, 30 and 40%, followed by their use in the follow-up experiments.

Compressive Strength of HBC

Figure 2 shows the low temperature compressive strength of HBC at curing temperatures of 30°C, 50°C, 70°C and 90°C. As can be observed, the strength of the cement stone increases with the curing temperature and curing age. This is due to the reason that an enhanced temperature increases the rate of the cement hydration, and the prolongation of the curing time makes the cement hydration more complete, thus, enhancing the strength. However, the absolute strength of the samples cured for 1 and 3 days is noted to be low. This is due to the reason that HBC possesses C_2S as the dominant mineral, and its hydration rate at low temperatures is slower than that of the conventional class G oil well cement (Cuesta et al., 2021).

Figure 3 shows the high-temperature compressive strength of HBC with and without quartz sand (B-0 to B-4 respectively represent 0–40% of quartz sand in HBC). The curing temperatures are 110°C, 150°C, 180°C, and 220°C. As observed from the figure, the overall strength of the cement stone decreases significantly on enhancing the temperature. The decline in the strength of pure HBC is noted to be the most serious (90%) after curing at 220°C as compared to 110°C. On increasing the amount of quartz sand, the decline in the strength of the cement stone is



significantly improved. For instance, HBC exhibits the highest strength and least decline at a quartz sand content of 40%. On curing at 220°C, the strength is observed to decline by 40%. After 7 days of curing, the compressive strength is noted reach 30 ± 0.5 MPa, and the strength recession phenomenon is significantly improved.

Phase Composition of HBC Hydration Products

Figure 4 shows the XRD pattern of HBC after low-temperature hydration for 7 days.

As observed from the figure, the main hydration products of pure HBC under low temperature curing are calcium hydroxide, C-S-H gel, calcium carbonate and periclase. There is no obvious difference in the types of the hydration products under different low temperature curing conditions, however, the strength of the diffraction peaks exhibits a change. The main diffraction peaks in the figure represent the presence of calcium hydroxide. As the temperature increases, the diffraction peaks of calcium hydroxide increase significantly, and the diffraction peaks of the other hydration products such as hydrated calcium silicate gel, calcium carbonate and periclase also increase to a certain extent. Therefore, as the temperature increases, the degree of cement hydration deepens, and the strength of the cement stone increases.

Figures 5, 6 present the XRD patterns of HBC with and without quartz sand after high temperature curing for 7 days.

According to **Figure 5**, the high temperature hydration products of pure HBC contain calcium hydroxide, dicalcium silicate hydrate, hydroxyl silicon calcium stone and C-S-H gel. However, as compared with the cement stone after low temperature curing, the cement stone after high temperature curing appears to be the hydroxyl silicon calcium stone. Almost no diffraction peaks of hydroxyl silicon calcium stone are observed in the cement stone cured at 110°C, however, strong diffraction peaks of the hydroxyl silicon calcium

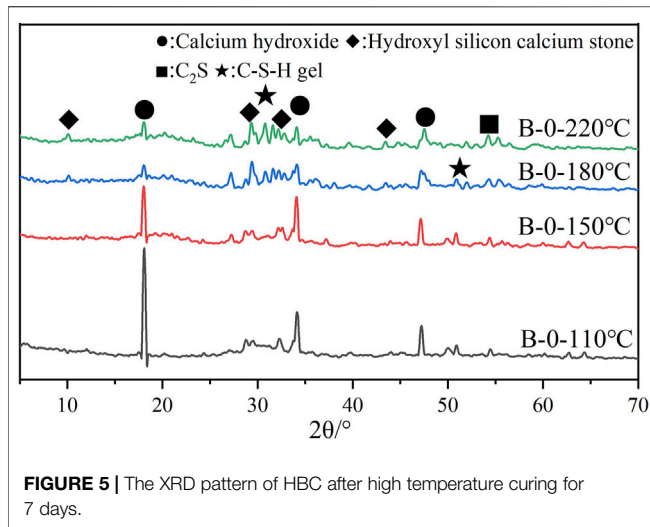


FIGURE 5 | The XRD pattern of HBC after high temperature curing for 7 days.

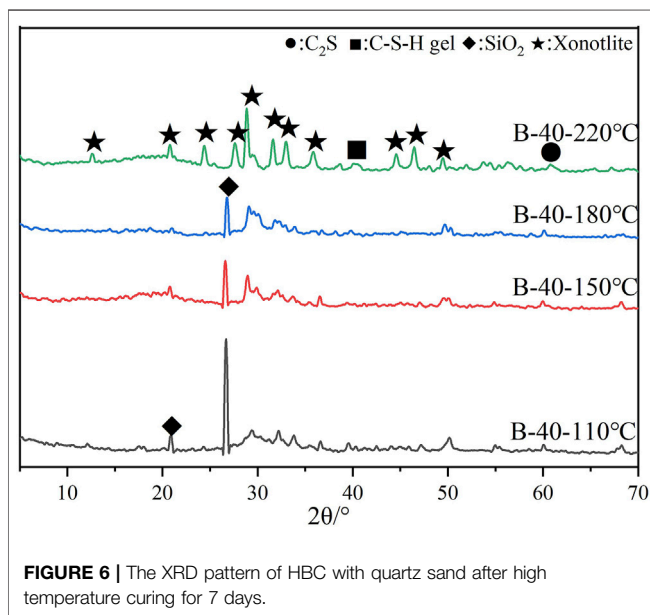


FIGURE 6 | The XRD pattern of HBC with quartz sand after high temperature curing for 7 days.

stone are noted in HBC cured at 180°C. On increasing the curing temperature, the calcium hydroxide content in HBC increases. This is due to the reason that the temperature significantly promotes the hydration reaction of the HBC cement and simultaneously makes the cement to produce products with a high calcium to silicon ratio. The phase composition of the high-temperature sanded cement hydrate is shown in **Figure 6**. As can be observed, after adding 40% quartz sand, xonotlite appears in the cement stone. Further, as the temperature increases, the diffraction peaks of xonotlite are strengthened, and the number of diffraction peaks gradually increases. On the other hand, the diffraction peak of silica is weakened. As the temperature rises to 220°C, the diffraction peak of silica is almost unobservable. This is owing to the reason that as the temperature increases, the reactivity of quartz sand is increased. As a result, and the consumption of silicon dioxide increases, which is more involved in the hydration reaction of cement.

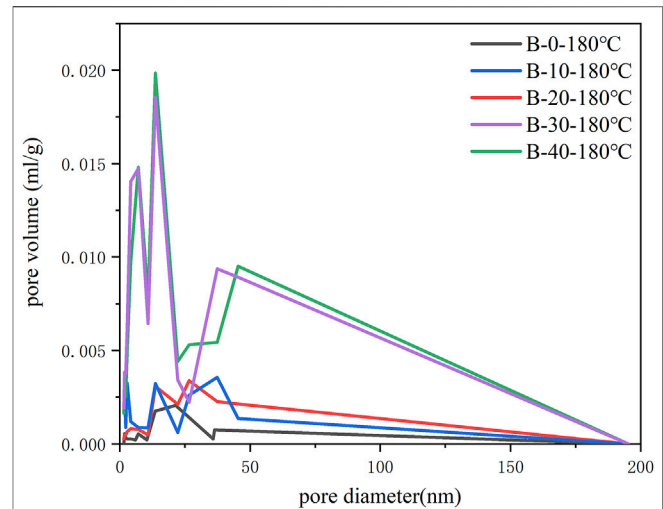


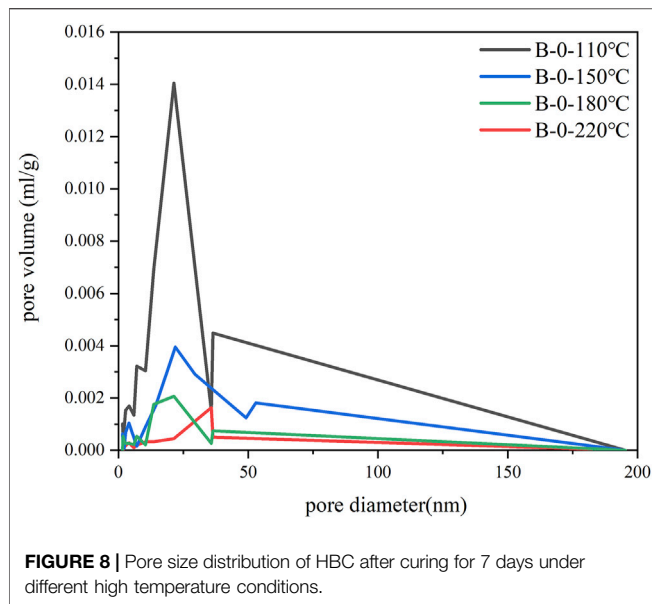
FIGURE 7 | Pore size distribution of HBC with different silica sand contents after curing at 180°C for 7 days.

The hydroxyl silicon calcium stone is a high-calcium silicate substance transformed from the C-S-H gel due to the calcium ion precipitation at high temperatures, which exhibits a negative effect on strength. Xonotlite reduces the calcium-silicon ratio of cement, especially leading to the accumulation and precipitation of the calcium ions. The resulting low-calcium silicate material is able to prevent its strength from declining (Churakov and Mandaliev, 2008). The findings from the phase analysis of the cement stone hydration products after mixing with quartz sand confirm this conclusion.

Pore Size Analysis of HBC

The pores with a pore diameter of less than 50 nm in the cement stone are classified as micropores and mesopores, which are conducive to the development of the cement stone strength. This is due to the reason that the pore size range of the C-S-H gel plays a major role in the strength of the cement stone. The pores with a pore diameter above 50 nm are termed as the harmful pores. The more are the harmful pores, the more unfavorable is the development of the cement stone strength (Wang et al., 2022).

Figures 7, 8 present the pore size distribution of HBC. As the temperature increases, the number of pores with a diameter less than 50 nm decreases. Thus, as the temperature rises, the C-S-H gel content in the cement stone is reduced, and the hydroxyl silicon calcium stone is formed. The structure of the cement stone is noted to be loose, thus, the strength of the cement stone decreases. With a gradual increase in the content of the quartz sand, the content of the hydroxyl silicon calcium stone in the cement stone decreases, leading to the formation of the fine xonotlite, thereby causing the number of favorable pores below 50 nm to increase sharply. At the same time, due to an increase in the amount of the quartz sand, the internal voids of the cement stone become large, thus, resulting in a certain increase in the number of the unfavorable pores above 50 nm. However, in general, the number of favorable pores in the cement stone after mixing with quartz sand is more than that of the harmful pores, which is conducive for the development of strength.



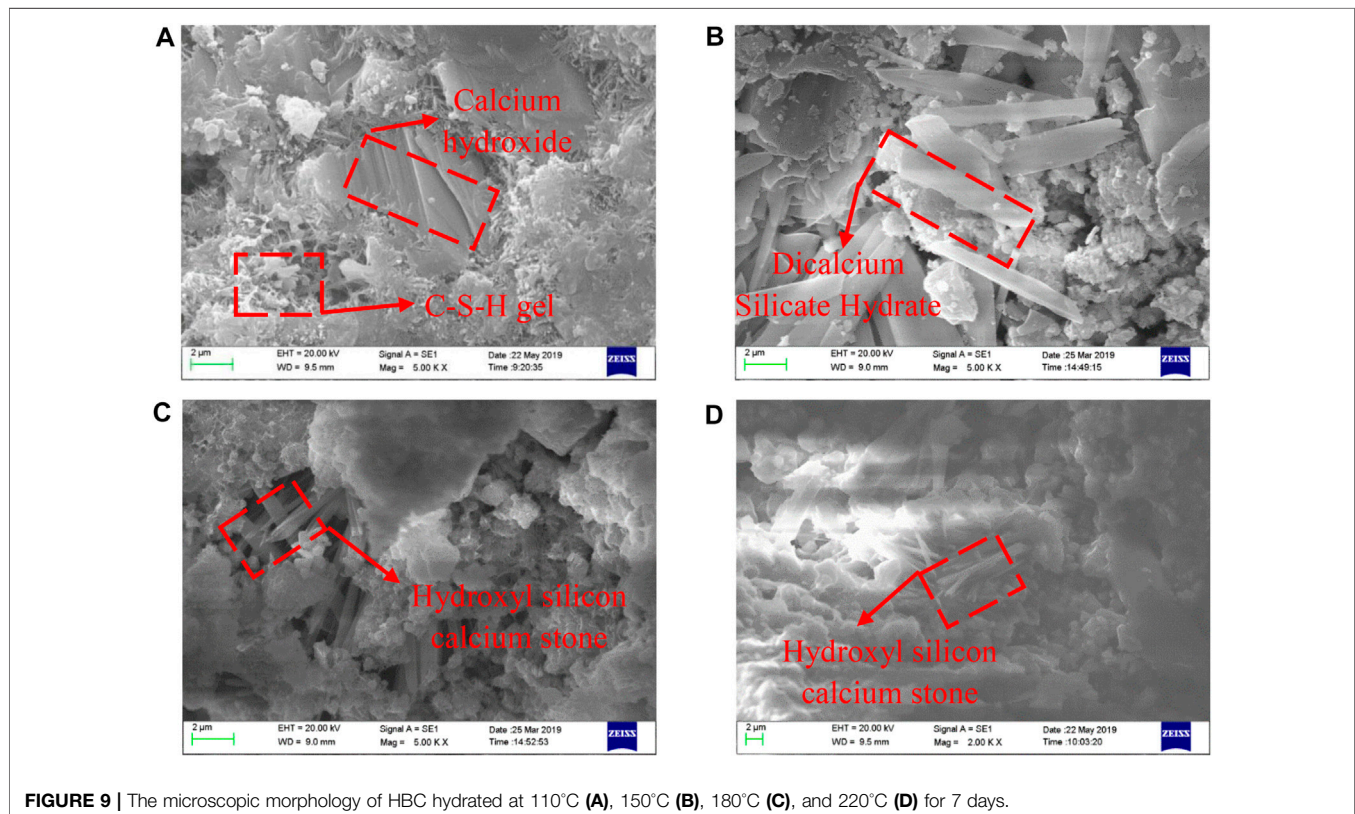
The Microstructure of HBC

Figure 9 shows the micro-morphology of pure HBC under different high temperature curing conditions.

The C-S-H gel with a network structure can be observed in the pure cement (**Figure 9A**) cured at 110°C (Zhao et al., 2021). The overall structure of the cement stone is also very dense, and the strength of the cement stone is high at this stage, with no

deterioration. The layered crystals embedded in the stone can also be observed, exhibited the presence of calcium hydroxide (Liu et al., 2018). However, as the temperature is increased, the plate-shaped dicalcium silicate hydrate is formed in the cement stone cured at 150°C. Its crystal density and crystallinity are noted to be high. A large number of pores are observed to exit the structure, thereby resulting in a low cement strength. On further increasing the curing temperature to 180°C, the hydroxyl silicon calcium stone is formed in the pure cement as clusters, which is caused by the further reaction of the dicalcium silicate hydrate. These crystals can still be observed in large quantities after curing at 220°C. This is also one of the main reasons contributing to the decline of the strength of the HBC cement stone (Koumpouri et al., 2021).

The SEM analysis of the materials is presented in **Figure 10**. **Figure 10A** reflects the microstructure of the cement with sand at 110°C, which is observed to be significantly different from the structure of the cement without sand. The hydration products are observed to contain the C-S-H gel and layered calcium hydroxide. As the curing temperature is increased, as shown in **Figures 10B,C**, xonotlite is no longer formed, however, a fine needle-like xonotlite is formed inside the cement stone. As the temperature is increased further, as shown in **Figure 10D**, the xonotlite content is also enhanced. Comparing the microscopic morphology of the pure HBC, it can be observed that the overall structure of the cement stone becomes dense after adding quartz sand, and the volume of xonotlite produced is smaller than that of the hydroxyl silicon calcium stone. It represents the main reason for the enhanced compactness and strength of the cement stone



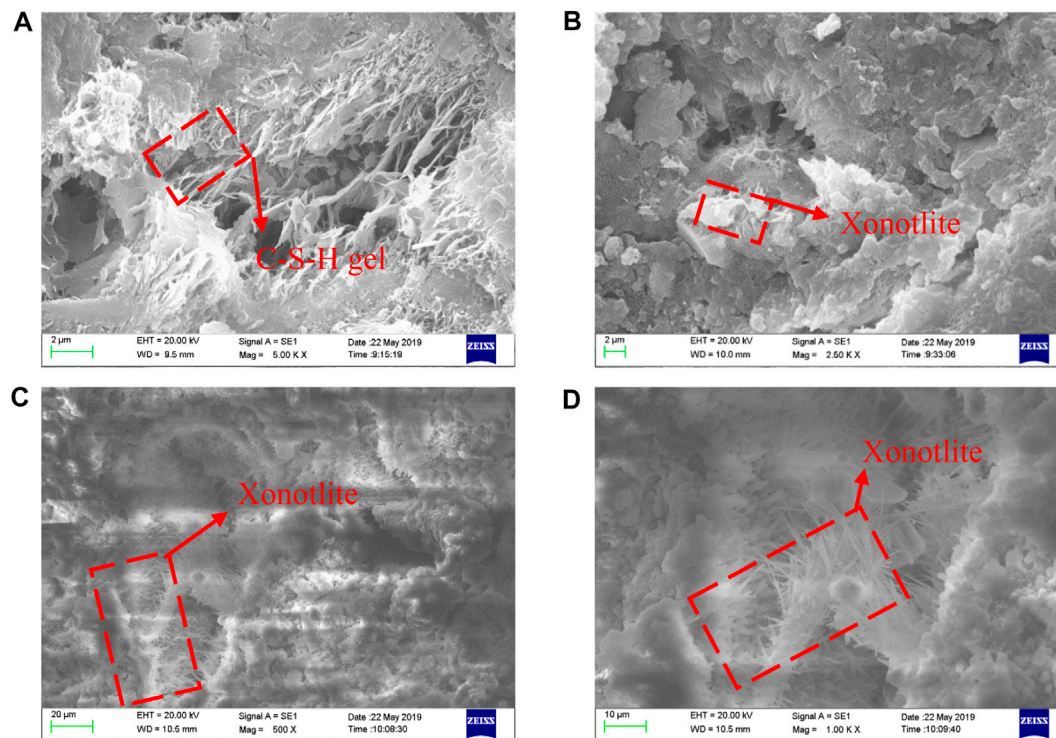


FIGURE 10 | The microscopic morphology of HBC mixed with 40% quartz sand at 110°C (A), 150°C (B), 180°C (C), 220°C (D) after hydration for 7 days.

structure. This is also confirmed by the findings from the phase analysis of the cement and stone (Xiawei et al., 2019).

CONCLUSION

This study uses quartz sand to delay the decline in the strength of the high belite cement at high temperatures. The high-temperature mechanical properties have been explored, and the corresponding mechanism has been analyzed through the microscopic characterization methods. The following conclusions can be drawn:

- 1) The mixing of quartz sand affects the engineering performance of the cement paste to a certain extent, resulting in poor fluidity and rheology.
- 2) The strength of the high belite cement does not decline at low temperatures. The strength of the pure cement declines significantly at high temperatures, and the mixing of quartz sand can delay its strength decline to a large extent.
- 3) The pure cement generates the hydrated dicalcium silicate and hydroxyl silicon calcium stone at high temperatures. After mixing with quartz sand, the overall structure becomes denser than the pure cement stone, with the appearance of the fine needle-shaped xonotlite.
- 4) The reason for the decline in the strength of the pure cement stone at high temperatures is the sharp reduction in the number of fine pores conducive for the strength development of the cement stone. However, the number of fine pores in the cement stone increases significantly after the addition of quartz sand, and

the formation of a large extent of the C-S-H gel and xonotlite delays the decline in its strength to a certain extent.

DATA AVAILABILITY STATEMENT

The original contributions presented in the study are included in the article/supplementary material, further inquiries can be directed to the corresponding author.

AUTHOR CONTRIBUTIONS

WZ and CX were responsible for proposing and checking the overall idea of the paper, XR and YJ were responsible for the preparation and test analysis of experimental materials, and NX was responsible for writing and revising the paper.

FUNDING

The authors appreciate the support of the CNOOC Limited Scientific Research Project “Ultra High Temperature and High Pressure Development Well Drilling and Completion Risk Assessment and Countermeasure Research” (No. YXKY-ZX-09-2021). The authors would also like to thank the Advanced Cementing Materials Research Center of SWPU for their kind assistance with the experiments.

REFERENCES

- Bahafid, S., Ghabezloo, S., Duc, M., Faure, P., and Sulem, J. (2017). Effect of the Hydration Temperature on the Microstructure of Class G Cement: C-S-H Composition and Density. *Cem. Concr. Res.* 95, 270–281. doi:10.1016/j.cemconres.2017.02.008
- Bu, Y., Du, J., Guo, S., Liu, H., and Huang, C. (2016). Properties of Oil Well Cement with High Dosage of Metakaolin. *Constr. Build. Mater.* 112, 39–48. doi:10.1016/j.conbuildmat.2016.02.173
- Churakov, S. V., and Mandaliev, P. (2008). Structure of the Hydrogen Bonds and Silica Defects in the Tetrahedral Double Chain of Xonotlite. *Cem. Concr. Res.* 38 (3), 300–311. doi:10.1016/j.cemconres.2007.09.014
- Cuesta, A., Ayuela, A., and Aranda, M. A. G. (2021). Belite Cements and Their Activation. *Cem. Concr. Res.* 140, 106319. doi:10.1016/j.cemconres.2020.106319
- Gong, Y., and Fang, Y. (2016). Preparation of Belite Cement from Stockpiled High-Carbon Fly Ash Using Granule-Hydrothermal Synthesis Method. *Constr. Build. Mater.* 111, 175–181. doi:10.1016/j.conbuildmat.2016.02.043
- Guo, S., Bu, Y., and Lu, Y. (2019). Addition of Tartaric Acid to Prevent Delayed Setting of Oil-Well Cement Containing Retarder at High Temperatures. *J. Pet. Sci. Eng.* 172, 269–279. doi:10.1016/j.petrol.2018.09.053
- Guo, S., Bu, Y., Zhou, A., Du, J., and Cai, Z. (2020). A Three Components Thixotropic Agent to Enhance the Thixotropic Property of Natural Gas Well Cement at High Temperatures. *J. Nat. Gas Sci. Eng.* 84, 103699. doi:10.1016/j.jngse.2020.103699
- Institute A P. API RP 10B-2 (2013). *Recommended Practice for Testing Well cements [S]*. Washington D.C: American Petroleum Institute publishing services.
- Jiang, C., Jiang, L., Tang, X., Gong, J., and Chu, H. (2021). Impact of Calcium Leaching on Mechanical and Physical Behaviors of High Belite Cement Pastes. *Constr. Build. Mater.* 286, 122983. doi:10.1016/j.conbuildmat.2021.122983
- Jiang, C., Jiang, L., Li, S., Tang, X., and Zhang, L. (2021). Impact of Cation Type and Fly Ash on Deterioration Process of High Belite Cement Pastes Exposed to Sulfate Attack. *Constr. Build. Mater.* 286, 122961. doi:10.1016/j.conbuildmat.2021.122961
- Koumpouri, D., Karatasios, I., Psycharis, V., Giannakopoulos, I. G., Katsiotis, M. S., and Kilikoglou, V. (2021). Effect of Clinkering Conditions on Phase Evolution and Microstructure of Belite Calcium-Sulpho-Aluminate Cement Clinker. *Cem. Concr. Res.* 147, 106529. doi:10.1016/j.cemconres.2021.106529
- Kuzielová, E., Žemlička, M., Másilko, J., and Palou, M. T. (2019). Development of G-Oil Well Cement Phase Composition during Long Therm Hydrothermal Curing[J]. *Geothermics* 80, 129–137. doi:10.1016/j.geothermics.2019.03.002
- Li, Y., Shi, T., and Li, J. (2016). Effects of Fly Ash and Quartz Sand on Water-Resistance and Salt-Resistance of Magnesium Phosphate Cement. *Constr. Build. Mater.* 105, 384–390. doi:10.1016/j.conbuildmat.2015.12.154
- Liu, H., Yu, Y., Liu, H., Jin, J., and Liu, S. (2018). Hybrid Effects of Nano-Silica and Graphene Oxide on Mechanical Properties and Hydration Products of Oil Well Cement. *Constr. Build. Mater.* 191, 311–319. doi:10.1016/j.conbuildmat.2018.10.029
- Liu, H., Bu, Y., Zhou, A., Du, J., Zhou, L., and Pang, X. (2021). Silica Sand Enhanced Cement Mortar for Cementing Steam Injection Well up to 380 °C. *Constr. Build. Mater.* 308, 125142. doi:10.1016/j.conbuildmat.2021.125142
- Shirani, S., Cuesta, A., Morales-Cantero, A., De la Torre, A. G., Olbinado, M. P., and Aranda, M. A. G. (2021). Influence of Curing Temperature on Belite Cement Hydration: A Comparative Study with Portland Cement. *Cem. Concr. Res.* 147, 106499. doi:10.1016/j.cemconres.2021.106499
- Standard C.N. GB/T 10238-2015 (2015). *General Administration of Quality Supervision, Inspection and Quarantine of the People's Republic of China and Standardization Administration of China*. Beijing, China: China Standards Press.
- Standard C.N. GB/T 19139-2012 (2012). *General Administration of Quality Supervision, Inspection and Quarantine of the People's Republic of China and China National Standardization Administration*. Beijing, China: China Standard Press.
- Sui, T., Fan, L., Wen, Z., and Wang, J. (2015). Properties of Belite-Rich Portland Cement and Concrete in China[J]. *Civil Eng. Archit.* 4 (9), 384–392. doi:10.17265/1934-7359/2015.04.002
- Vidal, A. V., Araujo, R. G. S., and Freitas, J. C. O. (2018). Sustainable Cement Slurry Using rice Husk Ash for High Temperature Oil Well. *J. Clean. Prod.* 204, 292–297. doi:10.1016/j.jclepro.2018.09.058
- Wang, C., Chen, X., Zhou, W., Wang, Y., Xue, Y., and Luo, F. (2019). Working Mechanism of Nano-SiO₂ Sol to Alleviate the Strength Decline of Oil Well Cement under High Temperature. *Nat. Gas Industry B* 6 (5), 517–523. doi:10.1016/j.ngib.2019.03.008
- Wang, C., Wang, L., Yao, X., Du, J., and Zhou, A. (2022). The Promoting Effect of Quercetin on Oil Well Cement Setting. *Constr. Build. Mater.* 317, 125689. doi:10.1016/j.conbuildmat.2021.125689
- Wei, T., Cheng, X., Gu, T., Huang, S., Zhang, C., Zhuang, J., et al. (2021). The Change and Influence Mechanism of the Mechanical Properties of Tricalcium Silicate Hardening at High Temperature. *Constr. Build. Mater.* 308, 125065. doi:10.1016/j.conbuildmat.2021.125065
- Xiawei, C., Xuezheng, Y., Chi, Z., Xianshu, G., Yongjin, Y., Kaiyuan, M., et al. (2019). Effect of Red Mud Addition on Oil Well Cement at High Temperatures[J]. *Adv. Cem. Res.* 33 (1), 1–40. doi:10.1680/jadcr.18.00224
- Zhao, W., Ji, X., Jiang, Y., and Pan, T. (2021). Effect of C-S-H Nucleating Agent on Cement Hydration. *Appl. Sci.* 11 (14), 6638. doi:10.3390/app11146638

Conflict of Interest: The authors WZ and XR are employed by CNOOC Research Institute Co. Ltd.,

The remaining authors declare that the research was conducted in the absence of any commercial or financial relationships that could be construed as a potential conflict of interest.

This research is under the overall responsibility of CNOOC Research Institute Co. Ltd., with the assistance of School of Safety and Ocean Engineering, China University of Petroleum (Beijing) and school of New Energy and Materials, Southwest Petroleum University. This research was funded by CNOOC Limited Scientific Research Project “Ultra High Temperature and High Pressure Development Well Drilling and Completion Risk Assessment and Countermeasure Research” (No. YXKY-ZX-09-2021). The fund's participation in this research was as follows: The fund provided support for research ideas, experimental equipment, materials, and funds for the research content of this article. The sponsor participated in the research design, data collection, analysis, interpretation, and the writing and submission of this article for publication.

Publisher's Note: All claims expressed in this article are solely those of the authors and do not necessarily represent those of their affiliated organizations, or those of the publisher, the editors and the reviewers. Any product that may be evaluated in this article, or claim that may be made by its manufacturer, is not guaranteed or endorsed by the publisher.

Copyright © 2022 Zhiqiang, Renjun, Jin, Xiucheng and Xiaowei. This is an open-access article distributed under the terms of the Creative Commons Attribution License (CC BY). The use, distribution or reproduction in other forums is permitted, provided the original author(s) and the copyright owner(s) are credited and that the original publication in this journal is cited, in accordance with accepted academic practice. No use, distribution or reproduction is permitted which does not comply with these terms.